

Published in final edited form as:

NMR Biomed. 2010 June ; 23(5): 523–531. doi:10.1002/nbm.1491.

Ferritin as a reporter gene for MRI: Chronic liver over expression of h-Ferritin during dietary iron supplementation and aging

Keren Ziv¹, Gila Meir¹, Alon Harmelin², Eyal Shimoni³, Eugenia Klein³, and Michal Neeman¹

¹Department of Biological Regulation, Weizmann Institute of Science, Rehovot 76100, Israel.

²Department of Veterinary Resources, Weizmann Institute of Science, Rehovot 76100, Israel.

³Department of Chemical Research Support, Weizmann Institute of Science, Rehovot 76100, Israel.

Abstract

The iron storage protein, ferritin, provides an important endogenous MRI contrast that can be used to determine the level of tissue iron. In recent years the impact of modulating ferritin expression on MRI contrast and relaxation rates was evaluated by several groups, using genetically modified cells, viral gene transfer and transgenic animals. This paper report the follow-up of transgenic mice that chronically over-expressed the heavy chain of ferritin (h-ferritin) in liver hepatocytes (liver-hfer mice) over a period of 2 years, with the aim of investigating the long-term effects of elevated level of h-ferritin on MR signal and on the well-being of the mice. Analysis revealed that aging liver-hfer mice, exposed to chronic elevated expression of h-ferritin, have increased R_2 values compared to WT. As expected for ferritin, R_2 difference was strongly enhanced at high magnetic field. Histological analysis of these mice did not reveal liver changes with prolonged over expression of ferritin, and no differences could be detected in other organs. Furthermore, dietary iron supplementation significantly affected MRI contrast, without affecting animal wellbeing, for both wildtype and ferritin over expressing transgenic mice. These results suggest the safety of ferritin over-expression, and support the use of h-ferritin as a reporter gene for MRI.

Keywords

ferritin; reporter gene; iron; aging

Introduction

Iron is an essential nutrient for the functionality and viability of cells. Due to its ability to mediate one-electron exchange reactions, iron participates in many metabolic pathways and is required for the proper function of numerous essential proteins such as the heme-containing proteins, electron transport chain and microsomal electron transport protein (1-3). However, this vital ability of iron may also be detrimental for living cells, as free radicals, which are potentially harmful to cells, may be generated through the Fenton reaction (that is, Fe-catalyzed hydroxyl radical production). Thus, maintenance of labile free iron homeostasis is highly important to the survival of animals, plants and microorganisms (1). Excess of free cellular iron activates the production of ferritin, which is a ubiquitous, highly conserved protein, that is responsible for controlled iron storage and release (2). Ferritin can store in its central cavity up to 4500 iron atoms as mineral ferrihydrite ($\text{Fe}_5\text{O}_3(\text{OH})_9$).

The MR properties of ferritin were the focus of extensive research and showed anomaly with high relaxivity at very low iron loading (4,5) and a peculiar linear rather than the expected quadratic dependence on the magnetic field (6). In recent years the possibility for use of ferritin as MR reporter gene was reported by a number of research groups (7-11). Based on the endogenous mechanisms for maintenance of labile iron homeostasis, along with the relatively high R_2 relaxivity of ferritin at low iron loading, we previously raised the hypothesis that overexpression of ferritin could augment R_2 relaxivity by redistribution of iron among more ferritin complexes as well as by increased total cellular iron level induction of expression of transferrin receptor (TfR) (4,7,8). The ability of the heavy chain of ferritin (h-ferritin), which possesses the ferroxidase activity, to act as MR reporter was first demonstrated in C6 glioma cells that were transfected with a tetracycline-inducible construct that carried h-ferritin. These cells were tested in vitro and showed a significant increase both in R_1 and R_2 . Inoculation of these cells in nude mice yielded tumors that showed significantly elevated R_2 (7). The use of ferritin as MR reporter was demonstrated also by infection of mice brain using adenovirus that encoded for both the heavy and light chains of human ferritin (10). The use of h-ferritin was further demonstrated with co-expression of transferrin receptor in neuronal stem cells that showed signal loss in T_2 and T_2^* weighted MR images in an iron enriched environment (9). Recent studies demonstrated the use of ferritin as MR reporter gene for labeling macrophages (12), monitoring of survival of mouse embryonic stem cells (11) for reporting of the activity of cyclic-AMP dependent protein kinase A by enzyme dependent aggregation (13), and for monitoring of gene transfer and expression in a tumor model (14,15).

The generation of TET-h-ferritin transgenic mice that over-express HA-tagged h-ferritin and enhanced green fluorescent protein (EGFP) in a tissue specific and tetracycline inducible manner opened the possibility for MR application of ferritin as a reporter gene in multiple organs and applications (8). In these mice tissue specific expression of ferritin is achieved by crossing with driver transgenic mice with expression of the tetracycline transactivator (tTA) regulated by the promoter of interest. Addition of tetracycline to the drinking water of double transgenic offspring mice suppresses expression of ferritin, and expression can be induced by tetracycline withdrawal. Endothelial selective expression was achieved using driver mice in which tTA expression is driven by the promoter of vascular endothelial (VE) cadherin (endothelial-hfer mice) (16,17). In these endothelial-hfer mice expression of ferritin resulted in elevation of R_2 , allowing detection of blood vessel induced expression in the brain of mature mice, as well as fetal vascular development detected non invasively in-utero.

In contrast to the expression of ferritin by endothelial cells which elevated R_2 as expected, liver hepatocyte expression of h-ferritin, using mice in which tTA was induced by the liver associated protein (LAP) promoter resulted in a more complicated effect on the MRI contrast. Surprisingly, young liver-hfer mice showed reduced R_2 upon acute expression of h-ferritin in liver hepatocytes. This effect was attributed to mild hepatic cytotoxicity leading to water vacuoles with low R_2 (8). Indeed previous studies showed varied response to elevated expression of h-ferritin ranging from protection of cells from reactive oxygen species (18,19), to regulation of free iron (20) and increased susceptibility to neurodegeneration in aging mice (21). The critical role of ferritin is further underscored by the in utero mortality of h-ferritin null mice, attributed to cardiac defects (22) and increased oxidative stress in brains of h-ferritin deficient mice (23). The phenotype observed for young liver-hfer mice is reminiscent of that previously reported for mice in which h-ferritin was elevated in response to deficiency in the iron regulatory protein-2 (24). Deposition and accumulation of iron is a well-known phenomenon of aging and was implicated in multiple pathologies such as Hemochromatosis (25), Alzheimer's disease (AD), and Parkinson's disease (26).

Since inertness is one of the most important characteristics that a reporter gene should possess, and in view of the fact that endothelial-hfer mice did not exhibit any pathology in utero and in adult, we pursued here the analysis of the impact of chronic elevated h-ferritin expression during aging of liver-hfer mice. The liver has a central role in iron homeostasis and ferritin storage. Given that iron overload is characterized by increased levels of ferritin, haemosiderin, and iron catalyzed lipid peroxidation we examined here the change in R_2 upon long-term overexpression of h-ferritin in liver hepatocytes in aging mice as well as the impact of prolonged over expression on increasing the capacity for iron storage during high iron diet.

Materials and Methods

Mice characterization

Animal experiments were approved by the Weizmann Institutional Animal Care and Use Committee. Transgenic LAP:tTA \times Tet:EGFP-HA ferritin double transgenic mice: Homozygous Tet:EGFP-HA ferritin mice (8) were mated with heterozygous LAP:tTA (liver associated protein) (27), double transgenic offspring (liver-hfer) over-express h-ferritin in liver hepatocytes. Wild type mice with matched genetic background (CB6F1; WT) were used as control. Ferritin expression was chronically induced in the double transgenic mice (no tetracycline).

Iron supplementation

MRI was applied for follow up of 4 groups of mice: WT mice and liver-hfer mice (with inducible transgene expression in hepatocytes) with high iron diet (2% carbonyl iron) and with normal diet (10 mice per group). 24 hours prior to each MRI scan the diet of all mice was replaced to regular diet in order to reduce artifacts associated with high iron content in the intestine.

Experimental timeline—The mice were treated with high iron diet from the age of 2 months for a period of 22 months. MRI scans at 4.7T, were performed when the mice were 5.5, 6.5, 8, 9, 20 and 24 months old. MRI scan at 9.4T was performed when the mice were 24 months old. Representative 20 months old mice were sacrificed and organs were taken for histological analysis. The study was completed when mice were 24 months old and liver sections were taken for assessment by electron microscopy. The same time points were used for mice that were treated with normal diet.

MRI studies

Mice anesthesia—i.p. injection of ketamine-xylazine mix (75 mg/kg Ketamine, Fort Dodge Animal Health, Fort Dodge, Iowa and 3 mg/kg Xylazine, VMD, Arendonk, Belgium).

MRI was acquired at horizontal 4.7T and 9.4T Bruker spectrometers using a birdcage coil. R_2 relaxation was measured using multi echo spin echo sequence with 8 echo times (TR= 2000 ms, TE= 11-88 ms, 2 averages, FOV 6X6 cm, 8 slices, in plane resolution 468 μ m, slice thickness 1 mm, matrix 128 \times 128, spectral width (SW) 50,000Hz).

R_2 values were derived by single exponential fit of the signal intensity decay with echo time ($I = I_0 e^{-TE \cdot R_2}$; MATLAB software, MathWorks, Inc. Hill Drive Natick, MA). Analysis included regions of interest (ROI) as well as pixel-by-pixel R_2 mapping.

Histopathological analysis

Following MRI analysis, multiple organs (brain, liver, heart, spleen and kidney) were retrieved for histological evaluation (stained at H&E and Prussian blue stains). Liver sections were also analyzed by electron microscopy.

Electron microscopy

Liver sections were examined by scanning electron microscope (SEM) and transmission electron microscope (TEM). For TEM studies the liver was sectioned with a razor blade and mounted in aluminum platelets with a depth of 100 μm , filled with 1-hexadecene (Sigma). The samples were then cryo-immobilized in an HPM 10 high pressure-freezing device (Bal-Tec, Liechtenstein). Freeze substitution was performed using a AFS2 freeze substitution device (Leica Microsystems, Vienna, Austria) in anhydrous acetone containing 2% glutaraldehyde for 3 days at -90°C and then warmed up to -30°C over 24 hours. The samples were washed with anhydrous acetone, infiltrated in a series of increasing concentration of Epon (Agar Scientific, UK) and polymerized at 60°C . Sections (60-80 nm in thickness) were obtained using an Ultracut UCT microtome (Leica Microsystems, Vienna, Austria). Unstained sections were examined in a Tecnai T12 electron microscope (FEI, Eindhoven, the Netherlands) operating at 120 kV. Images were recorded with an eagle $2\text{k} \times 2\text{k}$ CCD camera (FEI).

For SEM studies livers were placed overnight in 4% PFA, embedded in paraffin and sectioned to 10 μm sections that were placed on a carbon stab after paraffin removal using xylene. Images were taken with FEG ESEM, XL 30 form EFI, the regions that were rich in high atomic number elements were identified with a back scattered electrons detector (BSD) and were selected for element mapping. The X-ray maps were acquired with an energy dispersive X-ray detector (EDS) EDAX with ultra thin window. For Fe mapping the characteristic Kalpha line at 7.056 kV was used.

Results

High iron diet significantly elevates liver R_2

MRI (4.7T) was applied for dynamic follow up of R_2 relaxation in 4 groups of mice, including WT mice and liver-hfer mice (n=10 per group) subjected to either high iron diet or normal diet, during a period of 22 months (from 2 to 24 months of age; Figure 1). Under such chronic expression of h-ferritin, ROI analysis did not detect a significant difference in the average R_2 (at 4.7T) between liver-hfer and WT mice, neither for regular diet, nor for iron enriched diet (Figure 2A). Iron enriched diet led to a significant elevation in R_2 values for both WT and liver-hfer mice with no significant difference between WT and liver-hfer mice ($p < 0.05$ 2 tails un-paired Ttest; Figure 2A). Notably, all groups showed a significant rise in R_2 with age, which was steeper at early age for the iron-enriched diet and steeper at older age for the normal diet, but similar in both cases for the WT and liver-hfer groups.

Analysis of the spatial distribution of R_2 values derived from R_2 maps of mice fed with normal diet revealed that overexpression of h-ferritin resulted in a small increase in the fraction of voxels with high R_2 values (Figure 2B). These results are consistent with heterogeneous expression of the reporter by a subset of liver hepatocytes. In the presence of high iron diet the R_2 values were too high for derivation of reliable R_2 maps.

R_2 differences between liver-hfer and WT mice are elevated at high magnetic field (4.7T vs 9.4T)

Ferritin has a unique linear R_2 dependence on the magnetic field, which can be further enhanced by ferritin aggregation. The mice were scanned at two magnetic fields 4.7T and

9.4T when they were 2 years old. As expected for ferritin, the change in R_2 was strongly enhanced at high magnetic field revealing differences between the WT and liver-hfer mice fed normal diet (Figures 3A-D). R_2 values at 9.4T but not at 4.7T were significantly higher in normal diet liver-hfer mice compared to WT mice ($p < 0.05$ 2 tail unpaired Ttest, Figure 3E-F).

Histological analysis reveals differences in liver iron deposits between WT and liver-hfer mice

Liver sections were taken from representative mice after 18 months of treatment and stained with eosin & hematoxylin (H&E) and Prussian blue. H&E stain revealed similar vacuolar liver changes with aging in all mice groups (Figure 4A-B, E-F). Deposits of iron in the form of hemosiderin were observed in higher concentration only in liver-hfer mice (Figure 4B). High iron diet increased the hemosiderin concentration with clear difference between liver-hfer and WT mice (Figure 4E-F). The differences in iron content were evident in Prussian blue stain, which stains ferric ions (Fe^{+3}) (Figure 4C-D, G-H).

Over expression of ferritin in hepatocytes does not lead to pathological abnormalities

Brain, heart, kidney and spleen sections were retrieved from representative 20 months old mice and stained with eosin & hematoxylin (H&E) and Prussian blue. No pathological changes were noted in these organs with the chronic ferritin over expression (Figure 5 A-L). However, hemosiderin deposits were observed in the spleen of liver-hfer mice that were treated with normal iron diet but not in WT mice (figure 5 M-N). The difference in iron levels observed by H&E in the spleen of liver-hfer mice was confirmed also by Prussian Blue staining. High iron deposits were found in the kidney and spleen of liver-hfer mice compared to WT mice while treated with normal diet. Prussian blue staining was similar in the brain and heart of all groups (figure 6 A-H).

Electron microscopy analysis demonstrated the presence of ferritin and hemosiderin in liver-hfer mice subjected to a high-iron diet

Liver sections were examined by electron microscopy in order to verify the existence of iron and ferritin. SEM analysis was used to map iron in liver section (Figure 7). Regions that were rich in high atomic number elements were identified by back scattered electrons detector (BSD) and were selected for elements mapping. High iron levels were depicted in both WT and liver-hfer mice that were treated with high iron diet (Figure 7J-K), no such regions were observed in the livers of either WT or liver-hfer mice that were raised with normal diet (Figure 7 A, D). The presence of ferritin in liver hepatocytes was confirmed by TEM studies (Figure 8A, B), round structures at the size of 8-10nm are consistent with ferritin. In addition large hemosiderin clusters were observed in mice that were raised on high iron diet (arrows, Figure 8C, D).

Discussion

Reporter genes have become an indispensable tool for analysis of gene expression, protein interaction, cell lineage tracing and differentiation. Of particular interest are reporter mice, which can be used for analysis of development, disease and preclinical drug development, providing unique non invasive dynamic information on the genes or cells of interest while significantly reducing the number of animals required for a study (28). The use of reporter genes for the purpose of biological research and biomedical applications is always accompanied by the concern of side effects that may result from the introduction of a foreign gene. Thus, in the search for new reporter genes the critical properties include not only the specificity and sensitivity of the reporter gene but also the safety and inertness during prolonged expression.

Side effects of fluorescent reporters were evaluated for multiple settings including mouse bone marrow cells and cloned transgenic cattle (29)(30). Importantly, indirect side-effects can be associated with the site of insertion, as exemplified by the development of acute myeloid leukemia with EGFP expressing cells in rhesus macaques (31).

In recent years the use of ferritin as MR reporter gene was examined in several systems (7-10,13,14). The advantage of MRI includes its high endogenous anatomical and functional contrast and the ability to acquire high-resolution three dimensional information also in large organs not accessible for high resolution optical imaging. We previously reported the generation of transgenic reporter TET-ferritin mice, which express h-ferritin in a tissue specific and tetracycline inducible manner (8).

Initial assessment of young TET-ferritin mice included analysis of liver and endothelial specific expression. Endothelial-hfer mice revealed no pathologies (16), on the other hand, young mice that expressed h-ferritin in liver hepatocytes showed a transient mild hepatic cytotoxicity leading to vacuolar changes and reduced R_2 when h-ferritin expression was acutely induced by withdrawal of tetracycline. The study reported here aimed to evaluate the impact of chronic expression of ferritin by liver hepatocytes in normal husbandry conditions, and when challenged with high iron diet. Mice were monitored continuously over a period of two years.

In contrast to young mice that exhibited a transient reduction of R_2 values in response to acute h-ferritin overexpression in the liver (8), in older mice R_2 values increased compared to WT. While increased R_2 was marginally detectable at a magnetic field of 4.7T, as expected for ferritin, the difference in R_2 between WT and liver-hfer mice was significantly enhanced at 9.4T. The high field dependence of R_2 could stem from the heterogeneous pattern of transgene expression and iron accumulation. Such non-uniform distribution can lead to quadratic field dependence rather than linear (32,33).

Histo-pathological examination of liver-hfer and WT mice confirmed the increased iron content in the livers of transgenic mice, which was significant but was small relative to the physiological level of liver iron that can be achieved by feeding the mice with iron-enriched diet. In aging mice the vacuolar pattern in the liver was evident and similar for both liver-hfer and WT mice, for both normal and iron-enriched diets, suggesting that prolonged chronic over expression of ferritin does not alter baseline liver function, nor its capacity to respond to iron enriched diet. Histological evaluation of other organs including the brain, heart, spleen and kidney of liver-hfer mice revealed a normal phenotype. These results further substantiate the use of chronic expression of h-ferritin as a reporter gene for MRI analysis of liver hepatocytes. However, due to the central role of iron in multiple pathologies, each new application of ferritin should be carefully evaluated.

Acknowledgments

The Electron Microscopy studies were conducted at the Irving and Cherna Moskowitz Center for Nano and Bio-Nano Imaging at the Weizmann Institute of Science. This work was supported by the Minerva Foundation, by the European Commission 7th Framework ENCITE Integrated project and by 7th Framework European Research Council Advanced grant 232640-IMAGO (to MN). Michal Neeman is incumbent of the Helen and Morris Mauerberger Chair.

Abbreviations

h-ferritin	heavy chain ferritin
wt	wild type

tTA	tetracycline transactivator
LAP	liver associated protein
EGFP	enhanced green fluorescent protein
SEM	scanning electron microscope
TEM	transmission electron microscope
BSD	back scattered electrons detector
EDS	energy dispersive X-ray detector
SW	spectral width

References

- Arredondo M, Nunez MT. Iron and copper metabolism. *Mol Aspects Med.* 2005; 26(4-5):313–327. [PubMed: 16112186]
- Chiancone E, Ceci P, Ilari A, Ribacchi F, Stefanini S. Iron and proteins for iron storage and detoxification. *Biometals.* 2004; 17(3):197–202. [PubMed: 15222465]
- Siah CW, Trinder D, Olynyk JK. Iron overload. *Clin Chim Acta.* 2005; 358(1-2):24–36. [PubMed: 15885682]
- Gottesfeld Z, Neeman M. Ferritin effect on the transverse relaxation of water: NMR microscopy at 9.4 T. *Magn Reson Med.* 1996; 35(4):514–520. [PubMed: 8992201]
- Vymazal J, Brooks RA, Bulte JW, Gordon D, Aisen P. Iron uptake by ferritin: NMR relaxometry studies at low iron loads. *J Inorg Biochem.* 1998; 71(3-4):153–157. [PubMed: 9833320]
- Gossuin Y, Muller RN, Gillis P. Relaxation induced by ferritin: a better understanding for an improved MRI iron quantification. *NMR Biomed.* 2004; 17(7):427–432. [PubMed: 15526352]
- Cohen B, Dafni H, Meir G, Harmelin A, Neeman M. Ferritin as an endogenous MRI reporter for noninvasive imaging of gene expression in C6 glioma tumors. *Neoplasia.* 2005; 7(2):109–117. [PubMed: 15802016]
- Cohen B, Ziv K, Plaks V, Israely T, Kalchenko V, Harmelin A, Benjamin L, Neeman M. MRI detection of transcriptional regulation of gene expression in. *Nat Med.* 2007; 13(4):498–503. Epub 2007 Mar 2011. [PubMed: 17351627]
- Deans AE, Wadghiri YZ, Bernas LM, Yu X, Rutt BK, Turnbull DH. Cellular MRI contrast via coexpression of transferrin receptor and ferritin. *Magn Reson Med.* 2006; 56(1):51–59. [PubMed: 16724301]
- Genove G, DeMarco U, Xu H, Goins WF, Ahrens ET. A new transgene reporter for in vivo magnetic resonance imaging. *Nat Med.* 2005; 11(4):450–454. [PubMed: 15778721]
- Liu J, Cheng EC, Long RC Jr, Yang SH, Wang L, Cheng PH, Yang JJ, Wu D, Mao H, Chan AW. Noninvasive Monitoring of Embryonic Stem Cells in vivo with MRI Transgene Reporter. *Tissue Eng Part C Methods.* 2009
- Uchida M, Terashima M, Cunningham CH, Suzuki Y, Willits DA, Willis AF, Yang PC, Tsao PS, McConnell MV, Young MJ, Douglas T. A human ferritin iron oxide nano-composite magnetic resonance contrast agent. *Magn Reson Med.* 2008; 60(5):1073–1081. [PubMed: 18956458]
- Shapiro MG, Szablowski JO, Langer R, Jasanoff A. Protein nanoparticles engineered to sense kinase activity in MRI. *J Am Chem Soc.* 2009; 131(7):2484–2486. [PubMed: 19199639]
- Aung W, Hasegawa S, Koshikawa-Yano M, Obata T, Ikehira H, Furukawa T, Aoki I, Saga T. Visualization of in vivo electroporation-mediated transgene expression in experimental tumors by optical and magnetic resonance imaging. *Gene Ther.* 2009
- Ono K, Fuma K, Tabata K, Sawada M. Ferritin reporter used for gene expression imaging by magnetic resonance. *Biochem Biophys Res Commun.* 2009

16. Cohen B, Ziv K, Plaks V, Israely T, Kalchenko V, Harmelin A, Benjamin LE, Neeman M. MRI detection of transcriptional regulation of gene expression in transgenic mice. *Nat Med.* 2007; 13(4):498–503. [PubMed: 17351627]
17. Phung TL, Ziv K, Dabydeen D, Eyiah-Mensah G, Riveros M, Perruzzi C, Sun J, Monahan-Earley RA, Shiojima I, Nagy JA, Lin MI, Walsh K, Dvorak AM, Briscoe DM, Neeman M, Sessa WC, Dvorak HF, Benjamin LE. Pathological angiogenesis is induced by sustained Akt signaling and inhibited by rapamycin. *Cancer Cell.* 2006; 10(2):159–170. [PubMed: 16904613]
18. Pham CG, Bubici C, Zazzeroni F, Papa S, Jones J, Alvarez K, Jayawardena S, De Smaele E, Cong R, Beaumont C, Torti FM, Torti SV, Franzoso G. Ferritin heavy chain upregulation by NF-kappaB inhibits TNFalpha-induced apoptosis by suppressing reactive oxygen species. *Cell.* 2004; 119(4):529–542. [PubMed: 15537542]
19. Orino K, Lehman L, Tsuji Y, Ayaki H, Torti SV, Torti FM. Ferritin and the response to oxidative stress. *Biochem J.* 2001; 357(Pt 1):241–247. [PubMed: 11415455]
20. Cozzi A, Corsi B, Levi S, Santambrogio P, Biasiotto G, Arosio P. Analysis of the biologic functions of H- and L-ferritins in HeLa cells by transfection with siRNAs and cDNAs: evidence for a proliferative role of L-ferritin. *Blood.* 2004; 103(6):2377–2383. [PubMed: 14615379]
21. Kaur D, Rajagopalan S, Chinta S, Kumar J, Di Monte D, Cherny RA, Andersen JK. Chronic ferritin expression within murine dopaminergic midbrain neurons results in a progressive age-related neurodegeneration. *Brain Res.* 2007; 1140:188–194. [PubMed: 16631136]
22. Ferreira C, Bucchini D, Martin ME, Levi S, Arosio P, Grandchamp B, Beaumont C. Early embryonic lethality of H ferritin gene deletion in mice. *J Biol Chem.* 2000; 275(5):3021–3024. [PubMed: 10652280]
23. Thompson K, Menzies S, Muckenthaler M, Torti FM, Wood T, Torti SV, Hentze MW, Beard J, Connor J. Mouse brains deficient in H-ferritin have normal iron concentration but a protein profile of iron deficiency and increased evidence of oxidative stress. *J Neurosci Res.* 2003; 71(1):46–63. [PubMed: 12478613]
24. Grabill C, Silva AC, Smith SS, Koretsky AP, Rouault TA. MRI detection of ferritin iron overload and associated neuronal pathology in iron regulatory protein-2 knockout mice. *Brain Res.* 2003; 971(1):95–106. [PubMed: 12691842]
25. Fowler C. Hereditary hemochromatosis: pathophysiology, diagnosis, and management. *Crit Care Nurs Clin North Am.* 2008; 20(2):191–201. vi. [PubMed: 18424348]
26. Zandman-Goddard G, Shoenfeld Y. Hyperferritinemia in autoimmunity. *Isr Med Assoc J.* 2008; 10(1):83–84. [PubMed: 18300583]
27. Kistner A, Gossen M, Zimmermann F, Jerecic J, Ullmer C, Lubbert H, Bujard H. Doxycycline-mediated quantitative and tissue-specific control of gene expression in transgenic mice. *Proceedings of the National Academy of Sciences of the United States of America.* 1996; 93(20):10933–10938. [PubMed: 8855286]
28. Maggi A, Ottobrini L, Biserni A, Lucignani G, Ciana P. Techniques: reporter mice - a new way to look at drug action. *Trends Pharmacol Sci.* 2004; 25(6):337–342. [PubMed: 15165750]
29. Tao W, Evans BG, Yao J, Cooper S, Cornetta K, Ballas CB, Hangoc G, Broxmeyer HE. Enhanced green fluorescent protein is a nearly ideal long-term expression tracer for hematopoietic stem cells, whereas DsRed-express fluorescent protein is not. *Stem Cells.* 2007; 25(3):670–678. [PubMed: 17138958]
30. Liu Y, Wu Q, Cui H, Li Q, Zhao Y, Luo J, Liu Q, Sun X, Tang B, Zhang L, Dai Y, Li N. Expression of EGFP and NPTII protein is not associated with organ abnormalities in deceased transgenic cloned cattle. *Cloning Stem Cells.* 2008; 10(4):421–428. [PubMed: 18800861]
31. Seggewiss R, Pittaluga S, Adler RL, Guenaga FJ, Ferguson C, Pilz IH, Ryu B, Sorrentino BP, Young WS 3rd, Donahue RE, von Kalle C, Nienhuis AW, Dunbar CE. Acute myeloid leukemia is associated with retroviral gene transfer to hematopoietic progenitor cells in a rhesus macaque. *Blood.* 2006; 107(10):3865–3867. [PubMed: 16439674]
32. Jensen JH, Chandra R. Strong field behavior of the NMR signal from magnetically heterogeneous tissues. *Magn Reson Med.* 2000; 43(2):226–236. [PubMed: 10680686]

33. Jensen JH, Chandra R. Theory of nonexponential NMR signal decay in liver with iron overload or superparamagnetic iron oxide particles. *Magn Reson Med.* 2002; 47(6):1131–1138. [PubMed: 12111959]

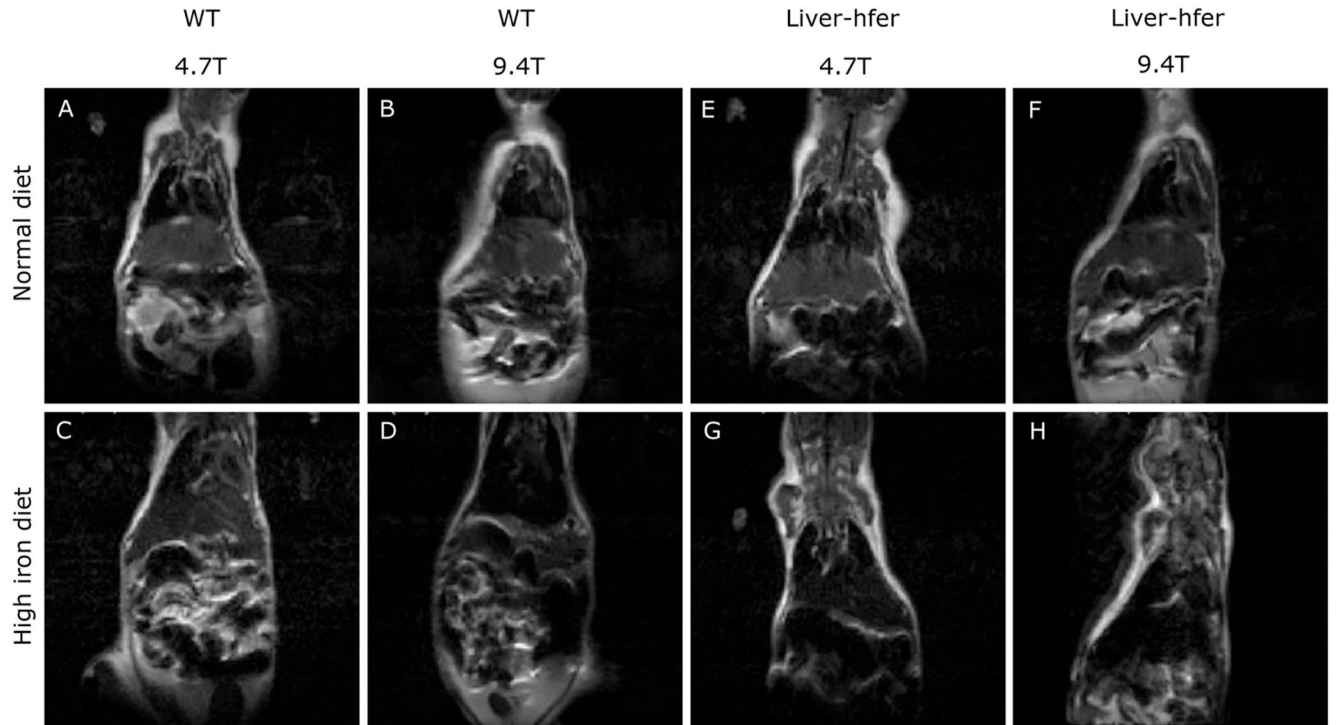


Figure 1. MRI gray scale image of mice with regular diet and High iron diet
4.7T and 9.4T MR images of WT mice (A-D) and liver-hfer mice (E-H) with constitutive transgene expression (2 years old) that were treated with normal diet and high iron diet (TR=2 s, TE=11 ms).

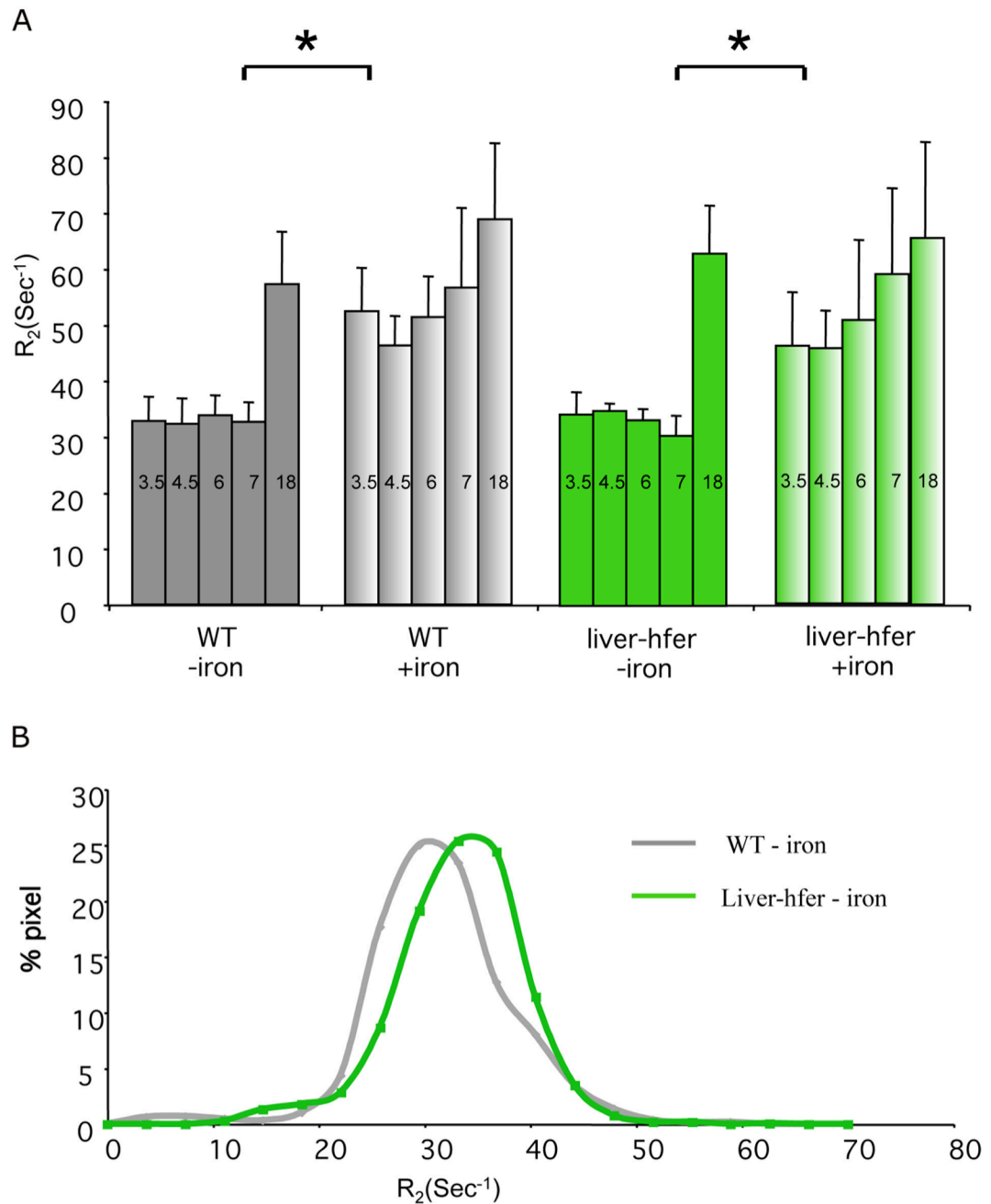


Figure 2. R₂ values according to ROI measurements in the liver of the different groups at 4.7T magnet

Each group was scanned at a 4.7T magnet during 18 months of normal and high iron diet, (A) ROI analysis showed significant difference in R₂ between the groups that were treated with high iron diet to groups with regular diet at all time points except for the last time point (*p<0.05 unpaired 2 tail Ttest). Numbers at the top of each bar state the mice age in months (iron supplementation diet was initiated when mice were 2 months old). (B) Analysis of the distribution of R₂ values derived from R₂ maps showed the spatial distribution of 4.7T R₂ values in the liver of 9 months old mice. Overexpression of h-ferritin resulted in elevated R₂ values. Wild type mice (gray), liver-hfer mice (green).

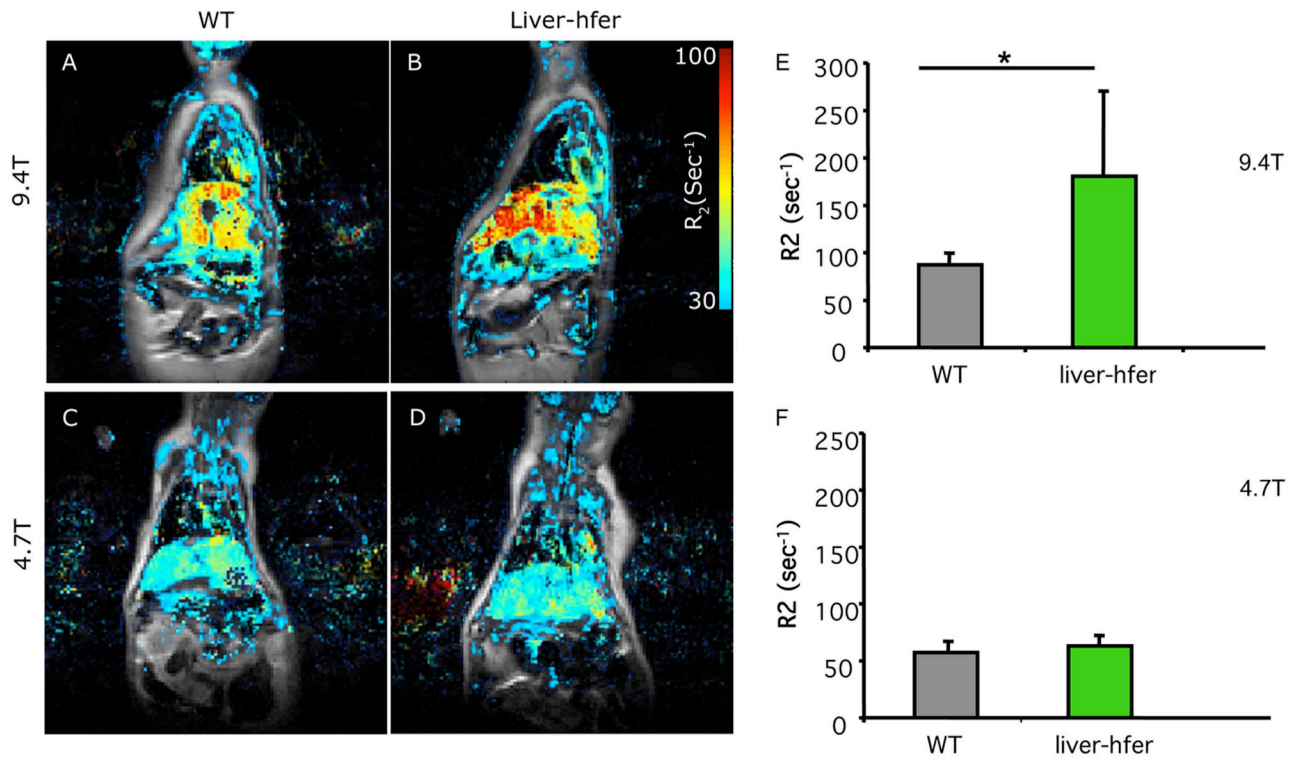


Figure 3. Field dependence of R₂ in liver-hfer mice

Overlay of R₂ color maps on a gray scale anatomical images (TE=6.4 ms) of WT mice (A, C) and liver-hfer mice (B, D) (age 24 months). Mice at the age of 24 months were imaged at two magnetic fields, 4.7T and 9.4T. (E, F) ROI analysis reveals significant difference in R₂ between WT and liver-hfer mice that were treated with regular diet and scanned at 9.4T (*p<0.05 unpaired 2 tail Ttest).

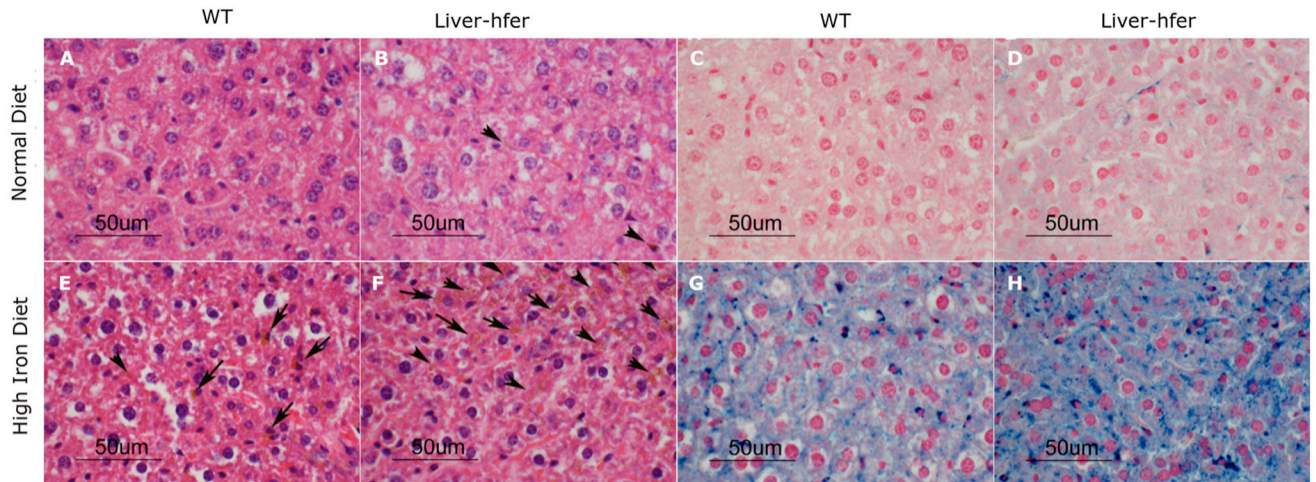


Figure 4. Histological evaluation of the liver

Liver sections that were taken from representative mice at the age of 20 months were stained with eosin hematoxylin (A-B, E-F) and by Prussian blue, which stains ferric ions (Fe+3) in bright blue color (C-D, G-H). (A, C) WT mice with normal diet, (B, D) liver-hfer mice with normal diet, (E, G) WT mice with high iron diet, (F, H) liver-hfer mice with high iron diet (arrows, hemosiderin deposits).

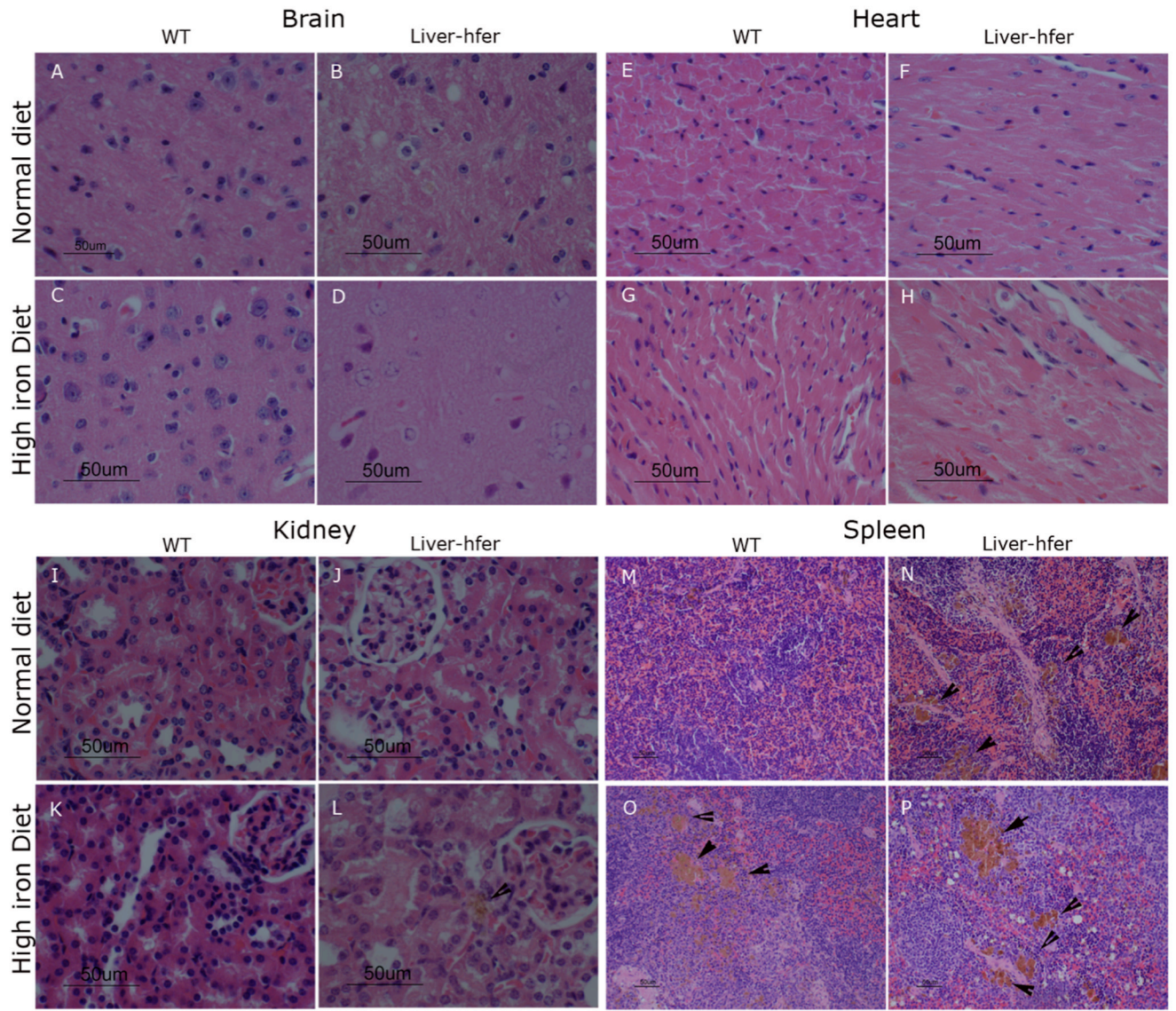


Figure 5. Histological evaluation of liver-hfer and WT mice

Different organs sections were taken from representative mice from each group at the age of 20 months and stained with eosin hematoxylin . (A-D) Brain, (E-H) Heart, (I-L) Kidney, (M-P) Spleen (arrows, hemosiderin deposits).

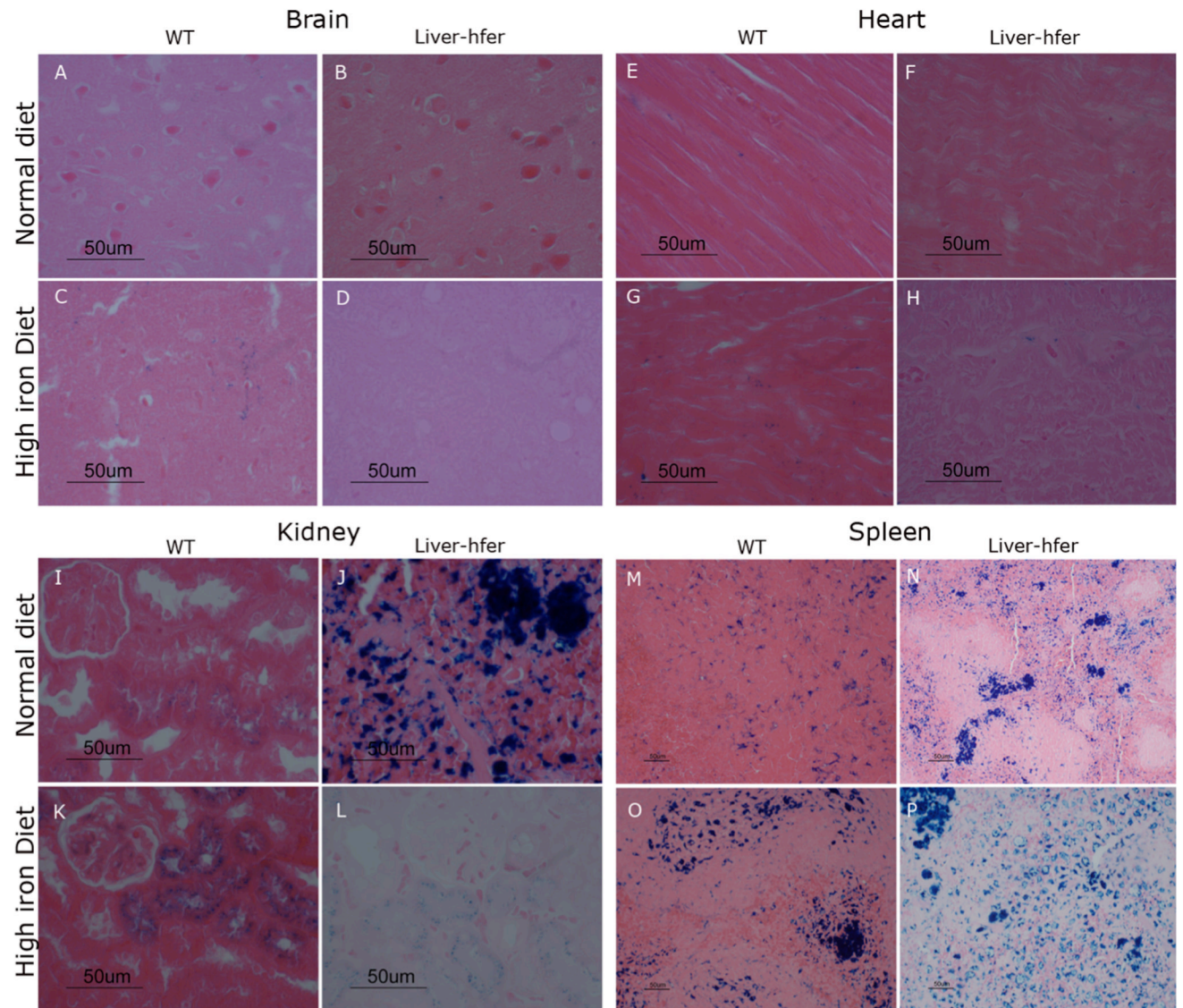


Figure 6. Iron levels evaluation by Prussian blue stain

Different organs sections were taken from representative mice from each group at the age of 20 months and stained by Prussian blue. (A-D) Brain, (E-H) Heart, (I-L) Kidney, (M-P) Spleen.

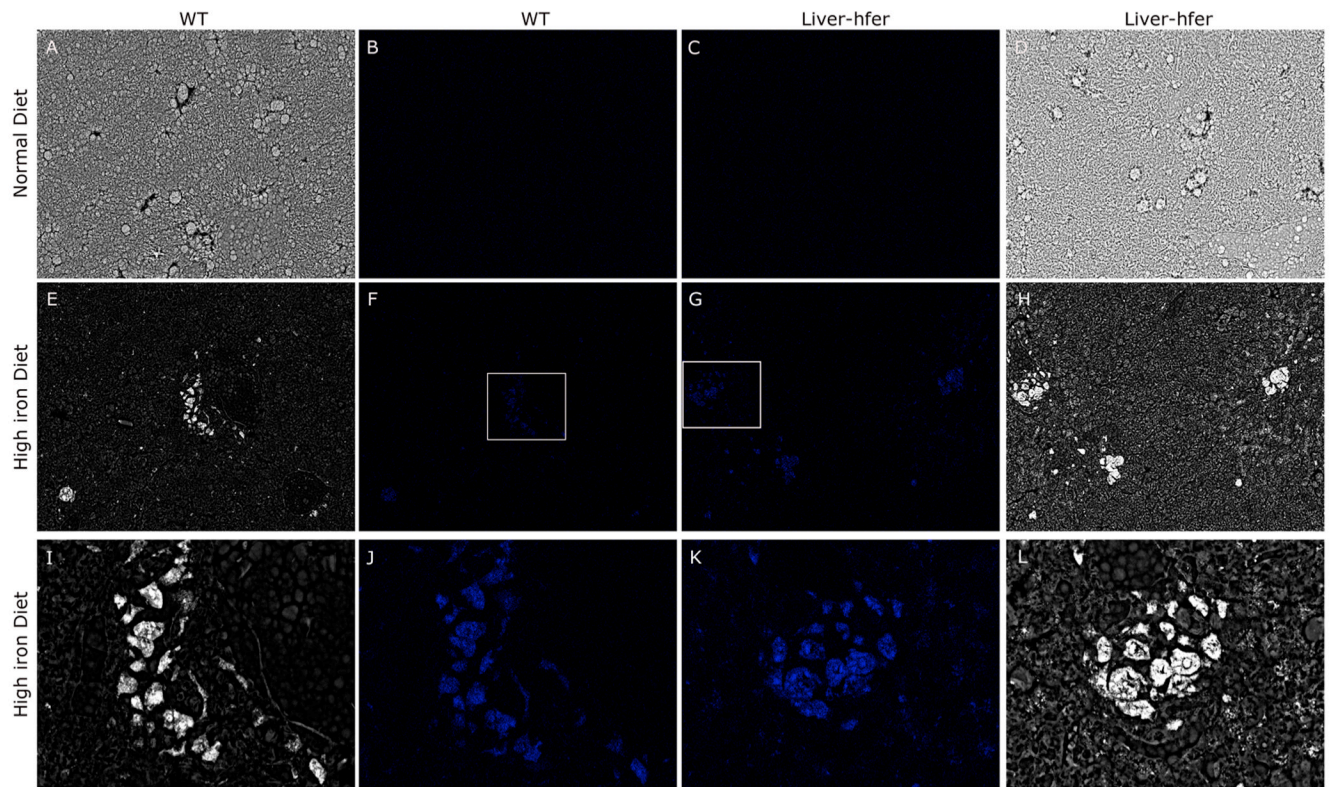


Figure 7. Iron mapping of the liver using scanning electron microscope (SEM)

Liver sections that were taken from representative mice at the age of 24 months were mapped for iron levels. (A-D) Livers of mice that were raised with normal diet (A, D back scattered images, B-C iron maps). (E-H) Livers of mice that were raised with high iron diet (E,H back scattered images, F-G iron maps). (I-L) magnification of the white square area. Scale bar for A-H equals 100 μ m, Scale bar for I-L equals 50 μ m.

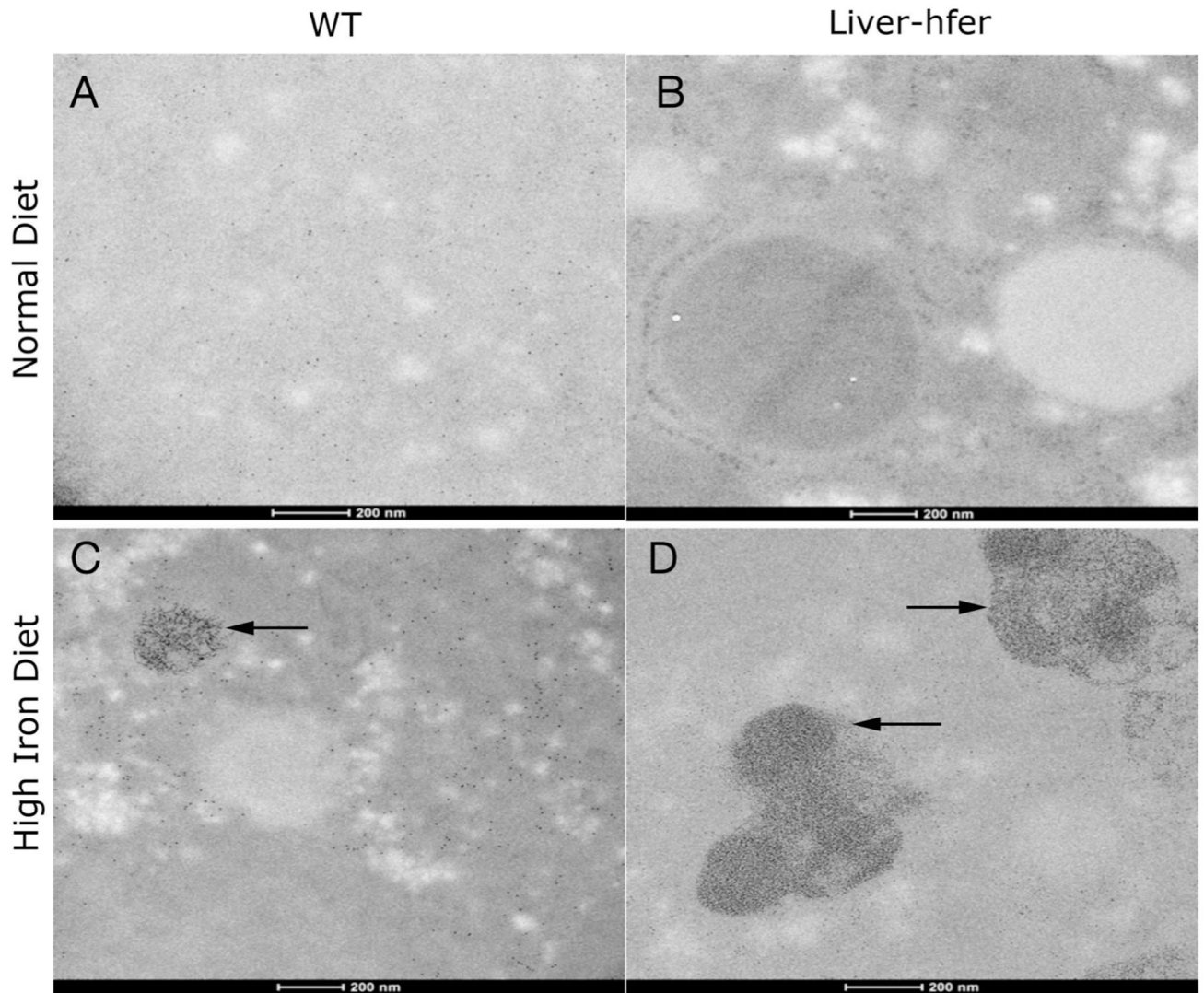


Figure 8. Transmission electron microscopy images of the liver

Liver sections that were taken from representative mice at the age of 24 months were examined by Transmission electron microscope. (A) WT mice with normal diet (B) liver-hfer mice with normal diet (C) WT mice with high iron diet (D) liver-hfer mice with high iron diet. Large hemosiderin clusters are observed in mice that were raised on high iron diet (C, D arrows marking). Scale bar equals 200nm.